Mon. Not. R. Astron. Soc. **322**, 231–246 (2001)

On the variation of the initial mass function

Pavel Kroupa★
Institut für Theoretische Physik und Astrophysik der Universität Kiel, D-24098 Kiel, Germany

Accepted 2000 September 12. Received 2000 August 24; in original form 2000

ABSTRACT

A universal initial mass function (IMF) is not intuitive, but so far no convincing evidence for a variable IMF exists. The detection of *systematic variations* of the IMF with star-forming conditions would be the *Rosetta Stone* for star formation.

In this contribution an average or Galactic-field IMF is defined, stressing that there is evidence for a change in the power-law index at only two masses: near $0.5\,M_\odot$ and near $0.08\,M_\odot$. Using this supposed universal IMF, the uncertainty inherent in any observational estimate of the IMF is investigated by studying the scatter introduced by Poisson noise and the dynamical evolution of star clusters. It is found that this apparent scatter reproduces quite well the observed scatter in power-law index determinations, thus defining the *fundamental limit* within which any true variation becomes undetectable. The absence of evidence for a variable IMF means that any true variation of the IMF in well-studied populations must be smaller than this scatter.

Determinations of the power-law indices α are subject to systematic errors arising mostly from unresolved binaries. The systematic bias is quantified here, with the result that the single-star IMFs for young star clusters are systematically steeper by $\Delta\alpha \approx 0.5$ between 0.1 and $1\,M_\odot$ than the Galactic-field IMF, which is populated by, on average, about 5-Gyr-old stars. The MFs in globular clusters appear to be, on average, systematically flatter than the Galactic-field IMF (Piotto & Zoccali; Paresce & De Marchi), and the recent detection of ancient white-dwarf candidates in the Galactic halo and the absence of associated low-mass stars (Ibata et al.; Méndez & Minniti) suggest a radically different IMF for this ancient population. Star formation in higher metallicity environments thus appears to produce relatively more low-mass stars. While still tentative, this is an interesting trend, being consistent with a systematic variation of the IMF as expected from theoretical arguments.

Key words: binaries: general – stars: formation – stars: kinematics – stars: luminosity function, mass function – globular clusters: general – open clusters and associations: general.

1 INTRODUCTION

Fundamental arguments suggest that the initial mass function (IMF) *should* vary with the pressure and temperature of the star-forming cloud in such a way that higher temperature regions ought to produce higher average stellar masses (Larson 1998). This is particularly relevant to the formation of Population III stars, because the absence of metals and the more intense ambient radiation field imply higher temperatures.

The IMF inferred from Galactic-field star-counts can be conveniently described by a three- or four-part power law (equations 1 and 2 below). The Galactic field was populated by many different star formation events. Given this well-mixed nature of the solar neighbourhood, present-day star formation ought to lead to *variations about the Galactic-field IMF*. In particular, a systematic difference ought to be evident between low-density environments (e.g., Taurus–Auriga and ρ Oph) and high-density regions (e.g., Orion nebula cluster, hereafter ONC), because above a certain critical density, star-forming clumps interact with each other before their collapse completes (Allen & Bastien 1995; Price & Podsiadlowski 1995; Murray & Lin 1996; Klessen & Burkert 2000). On considering the ratio between the fragment collapse time and the collision time-scale, and applying the analysis of Bastien (1981, his equation 8), it becomes apparent that the IMF in clusters similar to ρ Oph cannot be shaped predominantly through collisions between collapsing clumps. This is supported through the finding by Motte, André & Neri (1998) that the pre-stellar-clump MF in ρ Oph is similar to the observed MF for pre-main-sequence stars in ρ Oph. It is somewhat steeper than the Galactic-field IMF, especially if the binary systems that

★ E-mail: pavel@astrophysik.uni-kiel.de

must be forming in the pre-stellar cores are taken into account. Noteworthy is the fact that both the pre-stellar clump MF and the Galactic-field IMF have a reduction of the power-law index below about $0.5\,M_\odot$. In the core of the ONC, however, pre-stellar cores probably did interact significantly (Bonnell, Bate & Zinnecker 1998; Klessen 2001). Furthermore, once the OB stars ignite in a cluster such as the ONC, they have a seriously destructive effect through the UV flux, strong winds and powerful outflows, and so are likely to affect the formation of the least massive objects, including planets. This can happen, for example, through destruction of the accretion envelope, so that extreme environments like the Trapezium cluster may form a surplus of unfinished stars (brown dwarfs, hereafter BDs) over Taurus–Auriga. Luhman (2000) finds empirical evidence for this, but detailed dynamical modelling is required to exclude the possibility raised here that at least part of this difference may be due to the disruption of BD–BD and star–BD binaries in a dynamically evolved population such as the Trapezium cluster.

A conclusive difference has not been found between the IMF in Taurus–Auriga (Kenyon & Hartmann 1995; Briceno et al. 1998) and ρ Oph (Luhman & Rieke 1999) on the one hand, and the ONC (Palla & Stahler 1999; Muench, Lada & Lada 2000; Hillenbrand & Carpenter 2000) on the other. Similarly, Luhman & Rieke (1998) point out that no significant IMF differences for pre-main-sequence populations spanning two orders of magnitude in density have been found. Such conclusions rely on pre-main-sequence tracks that are unreliable for ages less than about 1 Myr (I. Baraffe, private communication), because the density, temperature and angular momentum distribution within the pre-main-sequence star is likely to remember the accretion history (Wuchterl & Tscharnuter 2000). Nevertheless, in support of the universal-IMF notion, it is remarkable how similar the Galactic-field MF is to the MF inferred for the Galactic bulge (Holtzman et al. 1998; Zoccali et al. 2000), again with a flattening around $0.5\,M_\odot$. Presumably star formation conditions during bulge formation were quite different from the conditions witnessed in the Galactic disc, but the bulge and disc metallicities are similar. Further related discussions on this topic can be found in Gilmore & Howell (1998).

The quest for detecting variations in the IMF has been significantly pushed forward by Scalo (1998), who compiled determinations of the logarithmic power-law index, Γ (equation 3), for many clusters and OB associations in the Milky Way (MW) and the Large Magellanic Cloud (LMC), which has about 1/5 to 1/3 the metallicity of the MW (e.g. Holtzman et al. 1997). While no systematic variation is detectable in a plot of Γ against stellar mass, m, between populations belonging to the two galaxies, a large constant scatter in Γ for stars more massive than $1\,M_\odot$ is evident instead. This raises the question of how large *apparent IMF variations* are due to small-number statistics and other as yet unexplored observational uncertainties, and whether this noise can mask, or even render undetectable, any true variations of the IMF.

Elmegreen (1999) shows that statistical variations of Γ, that are not dissimilar to the observed ones, result naturally from a model in which the Salpeter IMF constructs from random sampling of hierarchically structured clouds, if about $N = 100$ stars are observed. This model predicts that the scatter in Γ must decrease with increasing N.

In this contribution the reductionist philosophy is followed, according to which all non-star formation sources of *apparent variations* of the IMF must be understood before the spread of Γ can be interpreted as being due to the star formation process. To achieve this, an *invariant IMF is assumed* to study three possible contributions to the large scatter seen in the alpha-plot. **(i)** Poisson scatter due to the finite number of stars in a sample. This is similar to Elmegreen's approach, except that no explicit link to the distribution of gas clumps is made. **(ii)** Loss of stars of a preferred mass-scale as their parent star clusters evolve dynamically. This dynamical loss is not a simple function of stellar mass, because of the complex stellar-dynamical events in a young cluster. For example, while low-mass members preferably diffuse outwards as a result of energy equipartition, massive stars sink inwards where they meet and expel each other rather effectively. Finally, **(iiia)** wrong mass estimates because most stars are born in binary systems, and observers usually cannot resolve the systems. The simplest approach, taken here, is to replace the two component masses by the combined mass of the binary system, and to measure the system MF.

Issues also contributing to the scatter but not dealt with here are the following. **(iiib)** An observer infers the mass of a star from the observed luminosity incorrectly if the star is an unresolved binary, **(iiic)** wrong mass estimates from luminosities in the event of higher order multiplicities, which is a major bias for massive stars (e.g. Preibisch et al. 1999), **(iva)** stellar evolution and the application of incorrect pre-main-sequence and main-sequence evolutionary tracks, which corrupts the masses inferred from observed quantities as the stars evolve to or along the main sequence, and **(ivb)** incorrect estimates of stellar masses as a result of rapidly rotating massive stars and the use of non-rotating stellar evolution models. One issue to be stressed in this connection is that *stellar evolution* theory retains significant uncertainties (Kurucz 2000; Maeder & Meynet 2000; Heger & Langer 2000), which can only be reduced through continued attention.

The present study thus probably *underestimates* the scatter by focusing on points (i) to (iiia), but allows an assessment of the *fundamental limits* within which apparent IMF variations swamp true variations.

The *alpha-plot* and the form of the universal IMF adopted here are introduced in Section 2, and statistical variations of the power-law index are studied in Section 3. The star cluster models are described in Section 4, and Section 5 contains the results on the variation of the MF. In Section 6 the *dichotomy* in the alpha-plot and available evidence for a truly variable IMF are discussed. The conclusions are presented in Section 7.

2 THE ALPHA-PLOT AND THE GALACTIC-FIELD IMF

Observational data in the alpha-plot are used to infer a universal IMF.

2.1 The alpha-plot

Scalo (1998) combined available IMF estimates for star clusters and associations by plotting the power-law index, Γ (equation 3 below), against the mean $\log_{10} m$ of the mass range over which the index is measured (his fig. 5). Fig. 1 shows these *same data* by plotting the power-law index $\alpha = 1 - \Gamma$ against $\log_{10} m_{\rm av}$. The *alpha-plot* clearly shows the flattening of the IMF for $m \lesssim 0.5\,M_\odot$. It also shows no systematic difference between MW and LMC populations, as already shown by Massey, Johnson & Degioia-Eastwood (1995b) for massive stars. This is also verified for $0.6 \lesssim m \lesssim 1.1\,M_\odot$ by Holtzman et al. (1997), who use deep

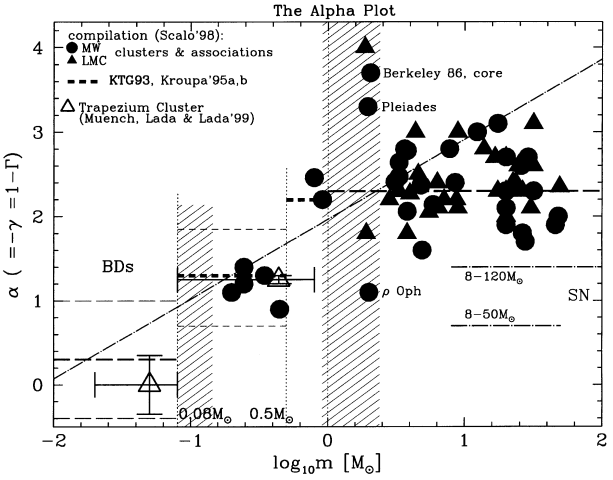

Figure 1. The *alpha-plot*. The data show the compilation by Scalo (1998) of determinations of α over different mass ranges for Milky Way (MW) and Large Magellanic Cloud (LMC) clusters and OB associations. Unresolved multiple systems are not corrected for. The large open triangles (Muench, Lada & Lada 2000 from Orion nebula cluster observations, binary corrections not applied) serve to illustrate the present knowledge for $m < 0.1\,\mathrm{M}_\odot$. The horizontal long-dashed lines in the BD regime are the Galactic-field IMF (equation 2) with associated approximate uncertainties. For $0.08 \leq m \leq 1.0\,\mathrm{M}_\odot$ the thick short-dashed lines represent the KTG93 single-star IMF (Kroupa, Tout & Gilmore 1993), which has $\alpha_3 = 2.7$ for $m > 1\,\mathrm{M}_\odot$ from Scalo's (1986) determination. The long-dashed lines for $m > 1\,\mathrm{M}_\odot$ show the approximate average $\alpha = 2.3$, which is adopted in the Galactic-field IMF (equation 2). The Miller & Scalo (1979) log-normal IMF for a constant star formation rate and a Galactic disc age of 12 Gyr is plotted as the diagonal long-dash-dotted line. The long-dash-dotted horizontal lines labelled 'SN' are those $\alpha_3 = 0.70(1.4)$ for which 50 per cent of the stellar (including BD) mass is in stars with 8–50(8–120) $\mathrm{M}_\odot$. The vertical dotted lines delineate the four mass ranges (equation 2), and the shaded areas highlight those stellar mass regions where the derivation of the IMF is additionally complicated due to unknown ages, especially for Galactic field stars: for $0.08 < m < 0.15\,\mathrm{M}_\odot$ long-contraction times make the conversion from an empirical LF to an IMF dependent on the precise knowledge of the age, and for $0.8 < m < 2.5\,\mathrm{M}_\odot$ post-main sequence evolution makes derived masses uncertain in the absence of precise age knowledge. A few of the MW data are labelled by their star clusters, and Table 1 lists the $m_{\rm av} < 1\,\mathrm{M}_\odot$ data.

Table 1. The data from Scalo's (1998) compilation with $m_{\rm av} < 1\,\mathrm{M}_\odot$.

$\log_{10} m_{\rm av}$	α	cluster	ref.
−0.70	1.10	ρ Oph	(Williams et al. 1995b)
−0.61	1.40	ρ Oph	(Comeron, Rieke & Rieke 1996)
−0.61	1.20	NGC 2024	(Comeron, Rieke & Rieke 1996)
−0.46	1.30	Praesepe	(Williams, Rieke & Stauffer 1995a)
−0.35	1.10	Pleiades	(Meusinger et al. 1996)
−0.10	2.46	ONC	(Hillenbrand 1997)
−0.04	2.20	Praesepe	(Williams, Rieke & Stauffer 1995a)

HST photometry for LMC fields and apply Monte Carlo models that include binary systems, various star formation histories (sfh) and metallicities, as well as observational errors.

The models discussed in Section 5 show that unresolved binary systems mostly affect the region $m \lesssim 1\,\mathrm{M}_\odot$, the data for which are listed in Table 1. Perusal of the references shows that only Meusinger, Schilbach & Souchay (1996) attempted a correction for unresolved binary systems. However, they adopted an artificial model of Reid (1991; see discussion in Kroupa 1995a), in which the binary proportion is only 40 per cent, half of which have similar companion masses. This is an unrealistic model (Kähler 1999), and leads to essentially no difference between the system and single-star luminosity functions (LFs) (fig. 7 in Meusinger et al. 1996; compare with fig. 11 in Kroupa 1995d). Their binary correction can thus be safely neglected.

2.1.1 $m > 3\,M_\odot$

For $m \gtrsim 3\,\mathrm{M}_\odot$ the data suggest that the Salpeter power-law value, $\alpha = 2.3$, is a reasonable fit over the whole range, as is also stressed by Massey (1998). Massey & Hunter (1998), for example, deduce that $\alpha \approx 2.3$ for $2.8 < m < 120\,\mathrm{M}_\odot$ in the massive cluster R136 in the LMC. This value is thus adopted throughout the rest of this paper, although notable examples of exotic clusters exist. The two massive, apparently young (2–4 Myr) Arches and Quintuplet clusters lying very close to the Galactic Centre (projected distance 30 pc) have $\alpha \approx 1.65$ (Figer et al. 1999), and the Galactic starburst template cluster NGC 3603 is found to have $\alpha \approx 1.7$ (Eisenhauer et al. 1998). Further work is desired to establish the exact nature of the central clusters, and clarify the age discrepancy between the low-mass and massive stars noted for NGC 3603, a problem possibly associated with pre-main-sequence models.

It is important to keep in mind that α may be systematically steeper than $\alpha = 2.3$ (or 1.7) due to unresolved binary systems, which are not usually corrected for in IMF estimates. The multiplicity proportion of massive stars is very high (Mason et al. 1998). For example, Preibisch et al. (1999) find that the OB stars in the well-studied ONC have, on average, 1.5 companions. For each primary, there is thus usually more than one secondary that adds at lower masses, steepening the observed IMF when corrected for. The effect depends on α, and Sagar & Richtler (1991) calculate that $\Delta\alpha = +0.34$ for $\alpha = 2.5$ and a binary proportion $f = 0.5$ (equation 5 below). If $f = 1$ (each massive primary has 1.0 companions), they obtain $\Delta\alpha = +0.40$. $\Delta\alpha$ is likely to be larger still, because each massive primary probably has more than one companion, typically. Since the empirical data in Fig. 1 implies an average $\alpha \approx 2.3$ for $m \gtrsim 3\,\mathrm{M}_\odot$, the true single-star IMF may in fact have $\alpha \approx 2.7$ (= 2.3 + 0.4), or even larger. A similar conclusion is reached by Scalo (1998, at the end of his section 4). Such corrections will not be removed if spectroscopic mass determinations are used instead of the inferior mass-estimates using photometry (Massey et al. 1995a), since unresolved systems will have similar effects on a spectroscopic sample.

In this paper the approximate average $\alpha = 2.3$ is adopted, with the aim of studying the effect of unresolved binary systems on the α inferred from the *system MF*, which an observer would deduce from the mixture of single stars and binary systems in a population resulting from star cluster evolution with initially $f = 1$. Because the assumptions (Section 4.3) imply that massive stars have very low-mass companions in this model, and because only binary systems are searched for in the data reduction software, the resulting model bias will be an underestimate. Further work is necessary to address this particular issue, which is also discussed further at the end of Section 3 and in Section 4.4.

The remarkable feature for $m \gtrsim 3\,\mathrm{M}_\odot$ in the alpha-plot is the *constant scatter*, and that the various power-law indices are distributed more or less randomly throughout the region $\alpha = 2.3 \pm 0.7$, without a significant concentration towards some value.

2.1.2 $0.8 < m < 3\,M_\odot$

The region for $0.8 \lesssim m \lesssim 3\,M_\odot$ shows an unusually large scatter. It is shaded because this particular mass range is problematical for a number of reasons.

Analysis of Galactic-field star-counts run into the difficulty that the age of the Galactic disc is comparable to the lifetime of these stars, so that stellar evolution corrections become very significant, but for this the sfh must be known (Scalo 1986; Haywood, Robin & Crézé 1997). That interesting constraints can be placed on the MW IMF using independently derived sfhs is shown by Maciel & Rocha-Pinto (1998), where the problems associated with the estimation of the field IMF for massive stars are documented.

The large spread of the cluster values in the region $0.8 \lesssim m \lesssim 3\,M_\odot$ may be due to the fact that the observed clusters have ages such that the stars in this mass range count to the most massive remaining in the clusters. They are thus subject to advanced stellar evolution and/or dynamical ejection from the cluster, because the most massive stars usually interact in the vicinity of the cluster core. Which of these is applicable is a sensitive function of the age of the cluster and the number of stars in it (more on this in Section 5.2). Finally, stellar evolution is by no means a solved subject for stars in this mass range (Dominguez et al. 1999) with remaining significant uncertainties. This compromises the conversion of stellar luminosity to mass. Ignoring the large scatter in this mass range, it can be seen that a single power-law index becomes applicable for $m > 0.5\,M_\odot$.

2.1.3 $0.1 < m < 1\,M_\odot$

The Galactic-field single-star IMF fits the data shown in Fig. 1 exceedingly well for $0.1 < m < 1\,M_\odot$ (that this agreement may be fortuitous though is shown in Section 6.2). In particular, it is remarkable that the data suggest a change in α near $0.5\,M_\odot$, as was initially derived from solar-neighbourhood star-counts by Kroupa, Tout & Gilmore (1991, hereafter KTG91), and later confirmed by Kroupa, Tout & Gilmore (1993, hereafter KTG93) and Kroupa (1995a) using a different mass–luminosity relation, a much more detailed star-count analysis including main-sequence and pre-main-sequence stellar evolution, and with different statistical tests. Similar work by Gould, Bahcall & Flynn (1997) using *HST* star-counts and Reid & Gizis (1997), who study a proposed extension of the nearby stellar sample to somewhat larger distances, also confirm these findings, as do Chabrier & Baraffe (2000), who estimate $\alpha \approx 1.2 \pm 0.1$ using the nearby volume-limited LF.

Of special importance is the mass range 0.5–1 $M_\odot$. The local sample of known stars is sufficiently large in this mass range that the nearby volume-limited LF is very well defined (Kroupa 2001a). Also, unresolved binaries do not significantly affect the LF in this mass range, because the stellar sample does not contain stars with $m > 1\,M_\odot$ that can hide lower mass companions. The mass–luminosity relation is also well understood for these stars, so that the MF determination should be accurate and precise. It is not surprising that the power-law slope has changed little over the decades (Salpeter 1955: $\alpha = 2.35$ for $0.4 < m < 10\,M_\odot$). From Fig. 1 an uncertainty of $\alpha = 2.3 \pm 0.3$ is adopted.

Unfortunately, the local sample of stars with $m \lesssim 0.5\,M_\odot$ is incomplete for distances larger than $d \approx 5$ pc, in contradiction to the belief by Reid & Gizis (1997), who use spectroscopic parallax measurements to extend their proposed volume-limited sample using previously known stars. Malmquist bias pollutes their sample by multiple systems that are much further away. The seriousness of the incompleteness of the nearby stellar census is shown by Henry et al. (1997), and is also pointed out by Chabrier & Baraffe (2000). This situation can *only* be improved with large-scale and deep surveys that find candidate nearby M dwarfs with subsequent *trigonometric* parallax measurements to affirm the distance, such that a *volume-limited sample* can be constructed. This will be possible through the upcoming astrometric space missions *DIVA* (Röser 1999) and *GAIA* (Gilmore et al. 1998). Being aware of this situation, the KTG studies combined the local ($d \leq 5.2$ pc) *volume-limited* sample with *flux-limited* deep photometric surveys, performing detailed Monte Carlo modelling of both Galactic-field samples. This *pedantic separation of the two star-count samples* is necessary, as completely different biases and errors operate. The result is the conservative uncertainty range of $\alpha = 1.3 \pm 0.5$ for 0.08–0.5 $M_\odot$ (KTG93). That the Galactic-bulge MF shows an indistinguishable behaviour to the Galactic-field MF in this mass range was already pointed out in Section 1.

2.1.4 $m < 0.08\,M_\odot$

For substellar masses the constraints have improved dramatically in the past few years as a result of the significant observational effort and instrumental advances. In the ONC, Muench et al. (2000) and Hillenbrand & Carpenter (2000) find $-1 \lesssim \alpha \lesssim 1$, although the pre-main-sequence tracks are unreliable at these ages. Similarly, in ρ Oph Luhman & Rieke (1999) estimate $\alpha \approx 0.5$, which is also found for IC 348 by Najita, Tiede & Carr (2000). In the Pleiades Cluster, Martin et al. (2000) estimate $\alpha \approx 0.53$, and for the solar neighbourhood, Reid et al. (1999) quote $1 \lesssim \alpha \lesssim 2$, whereas Herbst et al. (1999) estimate $\alpha < 0.8$ with 90 per cent confidence on the basis of no detections but accounting correctly for Galactic structure. For the time being, $\alpha = 0.3 \pm 0.7$ is a reasonable description of the IMF for BDs, and it will be shown in Section 5.2 that the observed MF depends sensitively on the dynamical age of the population.

The region 0.08–0.15 $M_\odot$ is shaded in Fig. 1 to emphasize the uncertainties plaguing Galactic-field star-count interpretations as a result of the long pre-main-sequence contraction times for these stars. As with the 0.8–3 $M_\odot$ region, the sfh must be known. The sfh has most recently been constrained by Rocha-Pinto et al. (2000).

2.2 The universal IMF

The available constraints can be conveniently summarized by the multiple-part power-law IMF (see Kroupa 2001b for details),

$$\xi(m) \propto m^{-\alpha_i} = m^{\gamma_i}, \tag{1}$$

where

$$\begin{aligned} \alpha_0 &= +0.3 \pm 0.7, \quad 0.01 \leq m/M_\odot < 0.08, \\ \alpha_1 &= +1.3 \pm 0.5, \quad 0.08 \leq m/M_\odot < 0.50, \\ \alpha_2 &= +2.3 \pm 0.3, \quad 0.50 \leq m/M_\odot < 1.00, \\ \alpha_3 &= +2.3 \pm 0.7, \quad 1.00 \leq m/M_\odot, \end{aligned} \tag{2}$$

and $\xi(m)\,\mathrm{d}m$ is the number of *single stars* in the mass interval m to $m + \mathrm{d}m$. The uncertainties correspond approximately to 99 per cent confidence intervals for $m \gtrsim 0.5\,M_\odot$ (Fig. 1), and to a 95 per cent confidence interval for 0.1–0.5 $M_\odot$ (KTG93). Below 0.08 $M_\odot$ the confidence range is not well determined.

Note that this form differs from Scalo's (1998) recommendation, mostly because the correct structure in the luminosity function below $1\,M_\odot$ is accounted for here. There is evidence for *only two changes in the power-law index*, namely near $0.5\,M_\odot$ and near $0.08\,M_\odot$. The frequently used Miller & Scalo (1979) IMF fails in the region 0.5–1 $M_\odot$, and especially for $m \gtrsim 5\,M_\odot$ (Fig. 1; see also Fig. 14 below). A useful representation of the IMF is achieved via the *logarithmic* form,

$$\xi_{\rm L}(m) = \xi(m) \ln 10m, \tag{3}$$

where $\xi_{\rm L}\,{\rm d}\log_{10} m \propto m^{\Gamma_i}\,{\rm d}\log_{10} m = m^{-x_i}\,{\rm d}\log_{10} m$ is the number of stars in the logarithmic mass interval $\log_{10} m$ to $\log_{10} m + {\rm d}\log_{10} m$.

The adopted IMF (equation 2) has a mean stellar mass $\langle m\rangle = 0.36\,M_\odot$ for stars with $0.01 \le m \le 50\,M_\odot$, and leads to the following stellar population: 37 per cent BDs (0.01–0.08 $M_\odot$) contributing 4.3 per cent to the stellar mass, 48 per cent M dwarfs (0.08–0.5 $M_\odot$) contributing 28 per cent mass, 8.9 per cent 'K' dwarfs (0.5–1.0 $M_\odot$) contributing 17 per cent mass, 5.7 per cent 'intermediate-mass (IM) stars' (1.0–8.0 $M_\odot$) contributing 34 per cent mass, and 0.37 per cent 'O' stars (>8 $M_\odot$) contributing 17 per cent mass.

A remarkable property of equation (2) is that 50 per cent of the mass is in stars with $0.01 \le m \le 1\,M_\odot$, and 50 per cent in stars with 1–50 $M_\odot$. Also, if $\alpha_4 = 0.70$ ($m > 8\,M_\odot$), then 50 per cent of the mass is in stars with $8 \le m \le 50\,M_\odot$, whereas $\alpha_4 = 1.4$ implies 50 per cent mass in 8–120 $M_\odot$ stars. These numbers are useful for the evolution of star clusters, because supernovae (SN) lead to rapid mass-loss which can unbind a cluster if too much mass resides in the SN precursors. This is the case in clusters that have $\alpha_3 = 1.80$: stars with $8 < m \le 120\,M_\odot$ contain 53 per cent of the mass in the stellar population! It is interesting that $\alpha \approx 1.8$ for $m \gtrsim 1\,M_\odot$ forms the lower bound on the empirical data in Fig. 1. However, even 'normal' ($\alpha = 2.3$) star clusters suffer seriously through the evolution of their $m > 1\,M_\odot$ stars (de La Fuente Marcos 1997).

3 PROCEDURE AND STATISTICAL VARIATION

One contribution to the scatter seen in the alpha-plot (Fig. 1) is Poisson noise. This can be studied by sampling N stars from the adopted IMF (equation 2), and studying the variation of α with N.

In order to construct synthetic alpha-plots, the following procedure is adopted. N masses are obtained by randomly sampling equation (2) with lower mass limit $m_{\rm l} = 0.01\,M_\odot$ and upper mass limit $m_{\rm u} = 50\,M_\odot$. This upper mass limit is chosen for consistency with the stellar-dynamical models (Section 4). The MF is constructed by binning the masses, m, into $30\log_{10} m$ bins which subdivide the range $-2.1 \le \log_{10} m \le +2.1$. Power laws are fitted using weighted linear regression (e.g. Press et al. 1994) to subranges that are defined as follows:

$$\begin{aligned}
&b1 \quad 6, \quad \log_{10}(0.01) < {\rm l}m \le \log_{10}(0.08),\\
&b2 \quad 6, \quad \log_{10}(0.08) < {\rm l}m \le \log_{10}(0.50),\\
&b3 \quad 4, \quad \log_{10}(0.40) < {\rm l}m \le \log_{10}(1.20),\\
&b4, \quad 4 \quad \log_{10}(1.00) < {\rm l}m \le \log_{10}(3.50),\\
&b5 \quad 4, \quad \log_{10}(3.00) < {\rm l}m \le \log_{10}(9.00),\\
&b6 \quad 8, \quad \log_{10}(5.00) < {\rm l}m,
\end{aligned} \tag{4}$$

where ${\rm l}m = \log_{10} m/M_\odot$, and the numbers, nb, behind the mass range number (e.g., $b1$) are the number of mass bins in the histogram in that particular mass range (e.g., $nb_1 = 6$). This subdivision ensures that the different mass regions in which α_i is known to be constant (equation 2) are not mixed up, but also allows studying the fitted α at values of lm where, for example, stellar evolution and/or dynamical effects are expected to be important. The result is $\alpha({\rm l}m_{\rm av})$, where l$m_{\rm av}$ is the average of lm over the nb_j ($j = 1, 6$) bins. In cases where the number of stars is too small, or the highest mass star is less massive than $10^{2.1}\,M_\odot$, some of the highest mass bins remain empty, causing l$m_{\rm av}$ in mass range $b6$ to vary between renditions.

The IMF is plotted together with two renditions using $N = 10^3$ stars in Fig. 2, to illustrate the procedure. The resulting alpha-plot is shown in Fig. 3 for many more renditions and different N. The input IMF is obtained essentially exactly for $N = 10^6$ and 10^5, verifying the procedure. The figure shows that deviations begin to

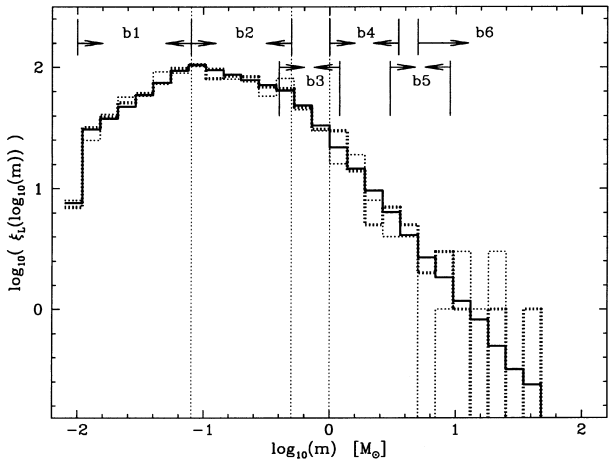

Figure 2. The adopted logarithmic IMF (equations 2 and 3), $\xi_{\rm L}/10^3$, for 10^6 stars (solid histogram). Two random renditions of this IMF with 10^3 stars are shown as the heavy and thin dotted histograms. The mass ranges over which power-law functions are fitted are indicated by the arrowed six regions (equation 4), while thin vertical dotted lines indicate the masses at which α_i changes.

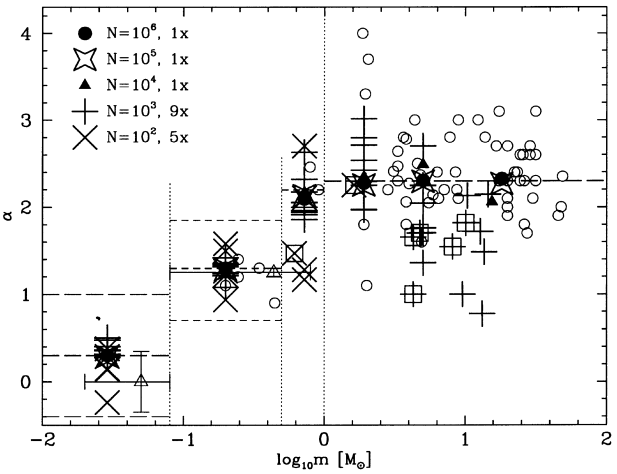

Figure 3. Purely statistical variation of α in the six mass ranges (equation 4) for different N as indicated in the key. Large outer squares indicate those α fits obtained with $nb = 2$ and 3 mass bins. The open circles, open triangles, vertical and horizontal lines are as in Fig. 1.

occur for $N = 10^4$ in the two highest mass ranges (*b*5 and *b*6), because these contain only a few per cent of N, i.e., a few hundred stars, spread over about 10 mass bins. For smaller N the scatter of $\alpha(\mathrm{l}m_{\mathrm{av}})$ becomes larger, with the average reproducing the IMF except when the MF is undersampled at large masses.

Fig. 2 illustrates this *sampling bias*. The undersampling of the histogram in the highest mass bins, when N is too small, leads to an apparent flattening of the MF in the most massive bins accessible to the stellar population, as is evident in Fig. 3. It is also evident in fig. 2 of Elmegreen (1999), and in typical star-count data, such as used by Massey et al. (1995b, their fig. 5) to infer the power-law index. Such samples contain typically a few dozen stars only (their table 5). This is interesting, possibly implying that the correct single-star IMF may be steepening, i.e., have an increasing α, with lm at the largest masses, since the uncorrected data suggest a constant α for $m \gtrsim 1\,\mathrm{M}_\odot$. This issue, together with the bias through the high multiplicity fraction, will require more explicit modelling of the biases affecting the observed IMF for massive stars.

In conclusion, Fig. 3 demonstrates that the observed scatter is arrived at approximately for populations that contain $10^2 \lesssim N \lesssim 10^3$ stars, which is quite typical for the type of samples available.

4 STAR CLUSTER MODELS

In Section 3, apparent variations of the IMF that result purely from statistical fluctuations are discussed. Additional sources of uncertainty are listed in the Introduction. Section 5 concentrates on quantifying the apparent variations that arise from stellar-dynamical effects and unresolved binary systems. To achieve this, a range of star cluster models are constructed. This approach is relevant to populations in young clusters, OB associations and even the Galactic field, because most stars form in embedded clusters (Lada & Lada 1991; Kroupa 1995b).

4.1 Codes

The dynamical evolution of the clusters studied here is calculated using NBODY6 (Aarseth 1999), which includes state-of-the-art stellar evolution (Hurley, Pols & Tout 2000), a standard Galactic tidal field (Terlevich 1987), and additional routines for initiating the binary-rich population (Kroupa 1995c). The N-body data are analysed with a large data-reduction program that calculates, among many quantities, the binary proportion and MFs.

4.2 The clusters

The cluster models are set up to have the same central density, $\rho_{\mathrm{C}} = 10^{4.8}\,\mathrm{stars\,pc^{-3}}$, as observed in the Trapezium cluster (McCaughrean & Stauffer 1994), giving a half-mass diameter crossing time $t_{\mathrm{cross}} = 0.24\,\mathrm{Myr}$. The centre of masses of the binary systems follow a Plummer density distribution (Aarseth, Hénon & Wielen 1974) with half-mass radius $R_{0.5}$. The average stellar mass is independent of the radial distance, R, from the cluster centre, and the clusters are in virial equilibrium. Their parameters are listed in Table 2. Cluster evolution is followed for 150 Myr.

4.3 The stellar population

Stellar masses are distributed according to the IMF (equation 2) with $m_{\mathrm{l}} = 0.01\,\mathrm{M}_\odot$ and $m_{\mathrm{u}} = 50\,\mathrm{M}_\odot$. This upper mass limit is half as large as the upper limit on the mass range used to evaluate the MF (equation 4), to take into account stellar mergers. Merging can occur during pre-main-sequence eigenevolution, as detailed below. The default models assume $\alpha_3 = \alpha_2$, but one model is also constructed with the possibly more realistic value $\alpha_3 = 2.7$ (this model has $\alpha_0 = 0.5$ for historical reasons).

Table 2. Cluster models: N and N_{bin} are the initial number of stars and binaries in each model (not taking into account mergers), $R_{0.5}$ is the half-mass radius, and $\langle m\rangle$ is the average stellar mass. The three-dimensional velocity dispersion is $\sigma_{3\mathrm{D}}$, and the median relaxation time is t_{rel}. Its range results from assuming $f = 1$ and $f = 0$, respectively, since f evolves. The number of calculations per model is N_{run}. Model B1E4d has $\alpha_3 = 2.7$ ($m > 1\,\mathrm{M}_\odot$; equation 2), whereas the other (default) models have $\alpha_3 = \alpha_2 = 2.3$. It took about 4 months to assemble these data on standard desktop computers.

model	N	N_{bin}	$R_{0.5}$ [pc]	$\langle m\rangle$ [$\mathrm{M}_\odot$]	$\sigma_{3\mathrm{D}}$ [$\mathrm{km\,s^{-1}}$]	t_{rel} [Myr]	N_{run}
B800	800	400	0.19	0.4	1.6	0.8–1.4	5
B3000	3000	1500	0.30	0.4	2.5	2.4–4.4	5
B1E4	10^4	5000	0.45	0.4	3.7	6.8–12.5	2
B1E4d	10^4	5000	0.45	0.3	3.2	7.9–14.5	2

Binaries are created by pairing the stars randomly. The binary proportion is

$$f = \frac{N_{\mathrm{bin}}}{N_{\mathrm{sing}} + N_{\mathrm{bin}}}, \tag{5}$$

where N_{sing} and N_{bin} are the number of single-star and binary systems, respectively. A birth binary proportion $f = 1$ is assumed. The initial mean system mass is $2\langle m\rangle$, with $\langle m\rangle$ being the average stellar mass. This results in an approximately flat mass-ratio distribution (fig. 12 in Kroupa 1995c). Note, however, that encounters in clusters lead to the preferred disruption of binaries with low-mass companions. The initially 'random' mass-ratio distribution evolves rapidly towards a distribution in which low-mass companions are less frequent, but still preferred (Kroupa 1995c). This is consistent with observations in that G-dwarf primaries (Duquennoy & Mayor 1991), Cepheids (4–9 $\mathrm{M}_\odot$; Evans 1995) and possibly OB stars (Mason et al. 1998; Preibisch et al. 1999) prefer low-mass companions.

Periods and eccentricities are distributed following Kroupa (1995c). The periods range from about 1 to 10^9 d, and *pre-main-sequence eigenevolution* changes the periods, mass ratios and eccentricities such that they are consistent with observational constraints for late-type main-sequence stars with short periods. Eigenevolution is the collective name for system-internal processes that evolve the orbital parameters, such as tidal circularization, mass transfer, and interactions with circumstellar and circumbinary discs. One feature of the pre-main-sequence eigenevolution model is that secondary companions gain mass during accretion if the periastron distance is smaller than a critical value. This affects the IMF by slightly reducing the number of low-mass stars, and slightly increasing the number of massive stars. Also, in some rare cases the binary companions merge giving $N_{\mathrm{sing}} > 0$, so that the true initial binary proportion is less than unity. Since only short-period binaries are affected by eigenevolution, the overall changes to the IMF are not significant.

The resulting single-star and system MFs are shown in Fig. 4. This figure demonstrates that the IMF that results from the eigenevolution model has a slightly smaller α, especially for $m < 0.5\,\mathrm{M}_\odot$

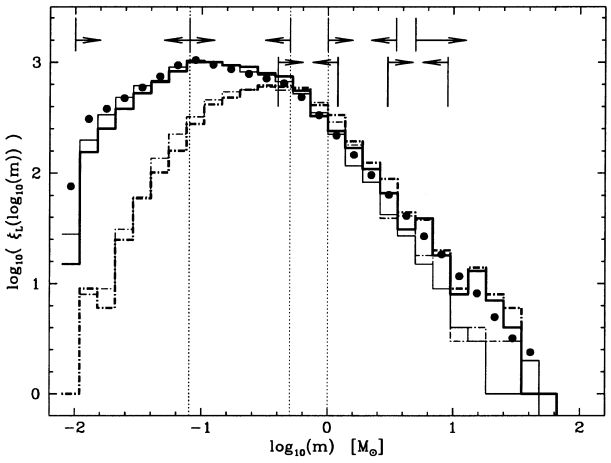

Figure 4. Mass functions for single stars (solid histograms) and systems (dot-dashed histograms) at $t = 0$ in models B1E4 (thick histograms) and B1E4d (thin histograms). Note the smaller number of massive stars in model B1E4d, which has a steeper IMF for $m > 1\,\mathrm{M}_\odot$ with $\alpha_3 = 2.7$ (Table 2). The solid dots are the IMF for $N = 10^6$ stars (Fig. 2) scaled to $N = 10^4$, and the vertical dotted lines and arrowed regions are as in Fig. 2.

(thick solid histogram). This effect is larger for the default case ($\alpha_3 = 2.3$), because the larger number of massive stars implies more systems in which the secondary gains mass as a result of eigenevolution. The effect on α is too small, however, to make a significant difference in the alpha-plot (e.g. Fig. 9 below). Fig. 4 also displays the large difference between the system MF and the single-star MF at low masses. The IMF has a maximum near $0.1\,\mathrm{M}_\odot$, whereas the system MF has one near $0.4\,\mathrm{M}_\odot$, and underestimates the number of 'stars' by an order of magnitude near $m = 0.01\,\mathrm{M}_\odot$, and by a factor of 3 near $m = 0.08\,\mathrm{M}_\odot$.

4.4 Nota bene

The *cluster models constructed here are extremes*, in that they have a very high central density equal to that observed in the ONC. This assumption leads to a *rapid depletion of the binary population*, as shown below (Fig. 6; see also de La Fuente Marcos 1997). Disruption of binaries occurs on a crossing-time scale (Kroupa 2000a) in any cluster, so that it takes much longer in real time for the binary population to decrease in a Pleiades-type cluster, for which Kähler (1999) shows that $f \approx 0.7$ is possible. Likewise, the pre-main-sequence cluster IC 348, which has a density of about $500\,\mathrm{stars\,pc}^{-3}$, has a binary proportion similar to that in the Galactic field (Duchene, Bouvier & Simon 1999). As shown by KTG91, such a binary proportion requires significant correction to the observed system LF to infer the IMF. The problem with unresolved binaries may still be even worse for lower density clusters, such as those studied by Testi, Palla & Natta (1999), because the binary population evolves on much longer time-scales, and is thus likely to be less evolved than in the clusters studied here. The problem will *never* be smaller in such clusters, unless they consist of a stellar population that had an unusually small initial binary proportion ($f < 0.3$), i.e., smaller than even in the evolved extreme models here. Such a population has never been observed in any Galactic cluster or association to this date (e.g. Ghez et al. 1997; Duchene 1999).

Any real population is thus likely to have a *larger binary proportion than in the models considered here* after about three crossing times ($\approx$0.8 Myr). In addition, the present results will be an underestimate of the bias, because only binary systems are considered. Real populations contain something like 20 per cent or more triple and quadruple systems, which, when not resolved, increase the systematic error made in the observational estimate of α. What is inferred in this paper is thus the *minimum correction to* $\boldsymbol{\alpha}$.

This is particularly true for $m \gtrsim 1\,\mathrm{M}_\odot$, because the observed mass-ratio distribution for massive stars (e.g. Preibisch et al. 1999) has secondaries that are typically more massive than $1\,\mathrm{M}_\odot$, whereas in the models here, massive primaries typically have very low-mass companions owing to the random sampling hypothesis. This is very important when considering the system MFs below. It will be evident that the models lead to essentially no bias for massive stars, but this is more likely to be a shortcoming of the present assumptions, rather than proving that the IMF for massive systems is not subject to a significant bias, as discussed in Section 2.1.1. Clearly, this is a fundamentally important topic requiring much more work to construct a more realistic initial mass-ratio distribution for massive stars. In addition, a systematically different IMF between the LMC and the MW for massive stars may become evident, *if* the binary properties differ systematically between the two galaxies, because then the correction for systematic bias would be different for the two samples. At present no such difference is known, and so the empirical LMC and MW data plotted in Fig. 1 can, at present, be taken only to mean that the IMF for massive stars may be the same in the two populations.

5 RESULTS

The results obtained from the stellar-dynamical calculations are used to study temporal and spatial apparent variations of the single-star and system MFs.

5.1 Cluster evolution

As an impression of the evolution of the star clusters, Fig. 5 displays the scaled number of *systems* and single stars with $R \leq 3.2\,\mathrm{pc}$. $N_{\rm sys}(t) = N_{\rm sing}(t) + N_{\rm bin}(t)$ increases for $t \lesssim 2.5\,\mathrm{Myr}$, because the disruption of binary systems liberates secondaries. That is, the observer would find that the number of 'stars' increases with time. After $t \approx 2.5\,\mathrm{Myr}$, $N_{\rm sys}$ decreases with a rate depending on N, because the clusters expand owing to binary-star heating, relaxation and mass-loss from evolving stars.

The binary proportion (Fig. 5) decreases within a few initial crossing times. The decay occurs on exactly the same time-scale for the different clusters, demonstrating that it is not the velocity dispersion in the cluster alone which dictates the disruptions, but the density as well. Owing to the ejection from the cluster of preferably single stars and because of mass segregation, f is larger for systems with $R \leq 3.2\,\mathrm{pc}$, and at times $t \gtrsim 2.5\,\mathrm{Myr}$, than for systems at larger distances from the clusters. The least massive clusters ($N = 800$) have expanded appreciably by this time, so that the remaining binary population in the cluster is hard, and no further significant disruption of binaries occurs ($f \approx 0.55$ and increasing for $t \gtrsim 2.5\,\mathrm{Myr}$). The more massive clusters, however, remain more concentrated for a longer time (top panel of Fig. 5), and consequently the binary-star hard/soft boundary remains at a higher binary binding energy for a longer time. At any time $t \gtrsim 3t_{\rm cross} \approx 0.7\,\mathrm{Myr}$, the binary proportion is higher in the clusters with smaller N, which is particularly evident in Fig. 6 below. This is a nice example of the caveat raised in Section 4.4. Further

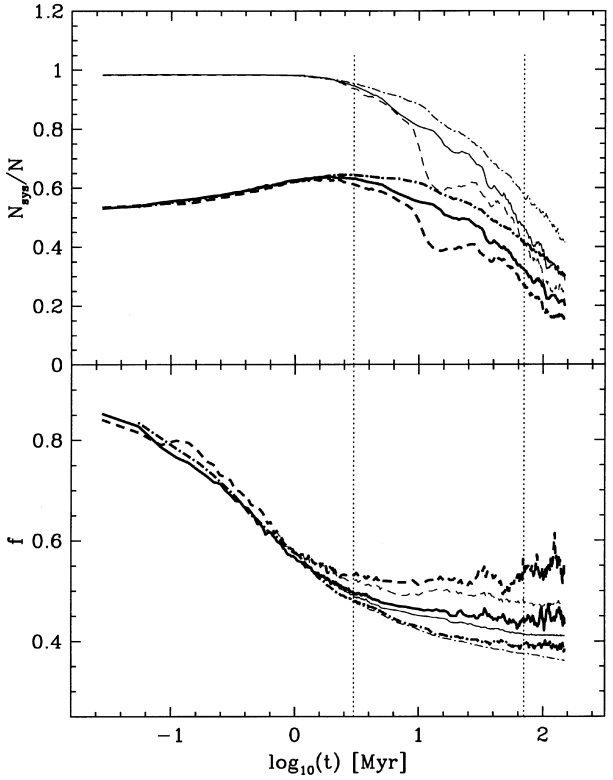

Figure 5. Examples of the evolution of individual clusters. **Top panel:** The number of systems (thick curves) and all individual stars and BDs (thin curves) within the innermost 3.2 pc. The short-dashed lines are for $N = 800$, the solid lines are for $N = 3000$, and the dot-dashed lines are for $N = 10^4$. **Bottom panel:** The binary proportion for $R \leq 3.2$ pc (thick curves), and all R (thin curves) for the same cases as in top panel. In both panels, the horizontal dotted lines indicate the times (3 and 70 Myr) at which the mass functions are observed.

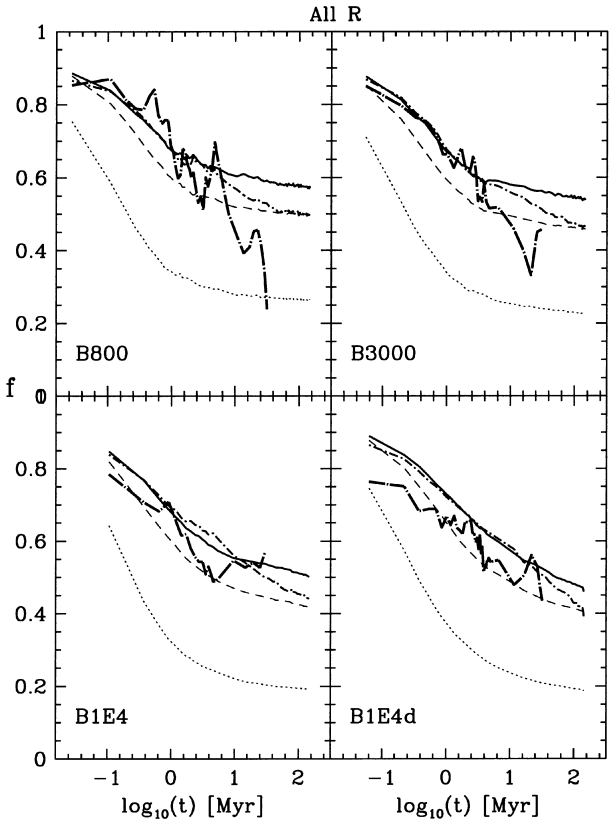

Figure 6. The proportion of binaries with primary masses $>8\,M_\odot$, f_O (thick long-dash-dotted curve), 1–8 $M_\odot$, f_{IM} (thin short-dash-dotted curve), and 0.5–1 $M_\odot$, f_K (solid curve). M dwarf primaries (0.08–0.5 $M_\odot$) have a binary proportion, f_M (thin dashed line), whereas brown dwarfs (0.01–0.08 $M_\odot$), f_{BD}, are shown as the thin dotted line. Each curve is an ensemble mean.

details on these processes are available in Kroupa (2000b), and in the seminal paper by Heggie (1975).

The evolution of the binary proportion for primaries with different masses is illustrated in Fig. 6. The binary proportion of BDs falls rapidly, and stabilizes near $f_{BD} = 0.20$ in all models. M dwarfs retain a much higher binary proportion by $t = 150$ Myr, $f_M \approx 0.4$–0.5, depending on N, and more massive primaries retain a slightly higher binary proportion still. The overall binary proportion of O primaries ($m \geq 8\,M_\odot$) shows a complex behaviour. Initially, most O primaries have low-mass companions. These are, however, exchanged for more massive companions near the cluster core. When the primaries explode, these companions are left or are ejected as single stars. In addition, violent dynamical encounters in the cluster core eject single massive stars. Overall, f_O decays, but higher order multiplicities that form in three-body encounters are not accounted for.

5.2 The alpha-plot for cluster populations

Having briefly discussed the evolution of the clusters and of the binary population, the following question can now be posed. What MFs would an observer deduce if an ensemble of such clusters were observed at different times, under the extreme assumption that the mass of each star or system can be measured exactly?

Figs 7 to 9 show the results for each N. The upper panels assume that the observer sees all stars with $R \leq 3.2$ pc, whereas in the lower panel it is assumed that only the system masses can be measured exactly for systems with $R \leq 3.2$ pc. The MFs are constructed at times $t = 0$, 3 and 70 Myr. For the single-star MFs, the results at $t = 0$ are the same as for pure statistical noise (Fig. 3).

At $t = 0$, the single-star IMF is well reproduced. The system MF, on the other hand, underestimates α significantly for $m_{sys} < 1\,M_\odot$, with $\alpha_0 \approx -0.8$ (instead of $+0.3$) for $m \lesssim 0.08\,M_\odot$, $\alpha_1 \approx +0.7$ (instead of $+1.3$) for $0.08 \lesssim m \lesssim 0.5\,M_\odot$, and $\alpha_2 \approx +1.5$ (instead of $+2.3$) for $0.5 \lesssim m \lesssim 1\,M_\odot$.

At $t = 3$ and 70 Myr, most of the BD systems have been disrupted (Fig. 6), with typically $f_{BD} \approx 0.2$, and most star–BD systems have also ceased to exist, so that α_0 is only slightly underestimated for the system MF. Work is in progress to study if the resulting mass-ratio distribution becomes consistent with the observed 'BD-companion desert' for nearby stars (M. Mayor 2000, private communication). In mass ranges $b2$ and $b3$, the power-law index is still underestimated significantly, because the surviving binary proportion is typically $f > 0.4$ for $m > 0.08\,M_\odot$. For $b2$ the lower panels in Figs 7 to 9 read $\alpha_1 \approx +0.8$, and for $b3$, $\alpha_2 \approx +1.7$. The bias in measuring $\alpha_{1,2}$ for the system MF rather than the single-star MF is thus not significantly reduced at later times.

This bias will operate for even older clusters, because further binary disruption is essentially halted in the expanded clusters, and f begins to increase with time as energy equipartition retains

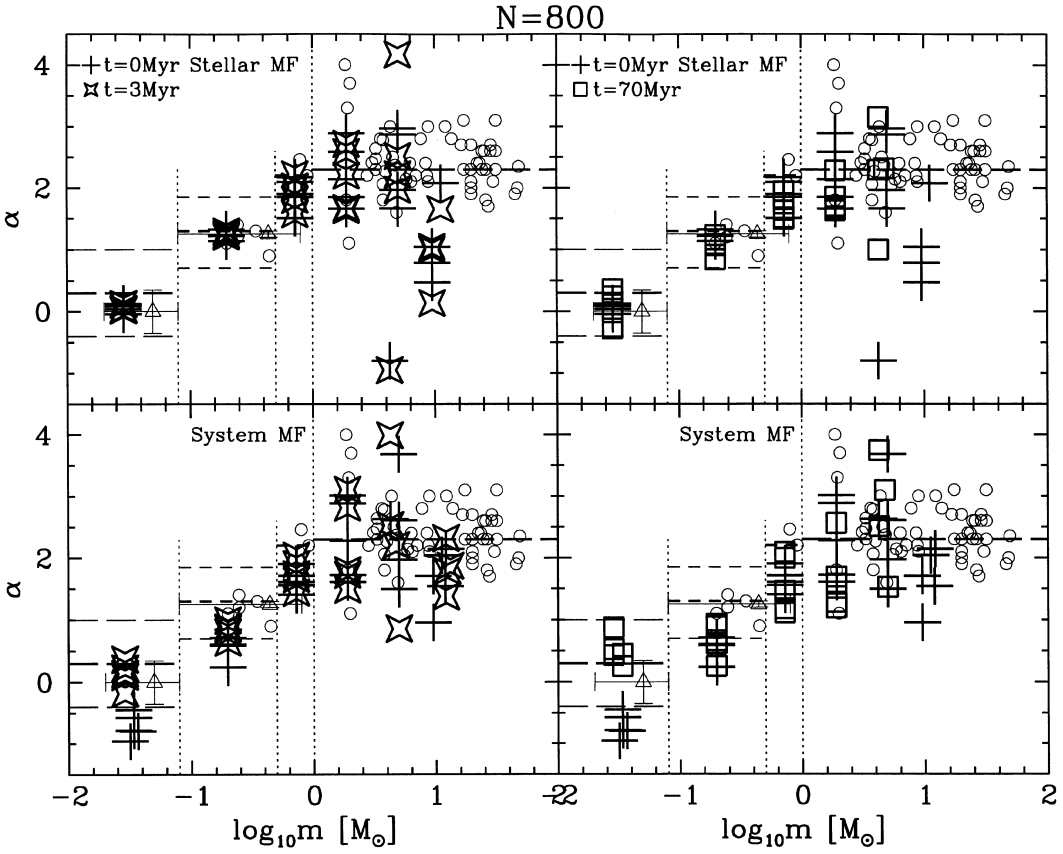

Figure 7. The α-plot for five B800 models at t = 0, 3 Myr (left panels) and 70 Myr (right panels). The single-star (upper panels) and system (lower panels) MFs are constructed for stars with R $\leq$ 3.2 pc. The open circles, open triangles, vertical and horizontal lines are as in Fig. 3.

the heavier binaries in the cluster at the expense of single stars (fig. 3 in Kroupa 1995d). However, with time the bias will decrease for α_2 as the turn-off mass becomes smaller, i.e., as the number of primaries with $m \gtrsim 1\,\mathrm{M}_\odot$ decreases. As an extreme example, globular clusters retain a significant proportion of their low-mass stars (Vesperini & Heggie 1997), but stars with $m \gtrsim 0.8\,\mathrm{M}_\odot$ have ceased to exist, so that no $m \lesssim 0.8\,\mathrm{M}_\odot$ companions are 'hidden' by brighter primaries.

For $N = 800$ (Fig. 7) the scatter in range $b5$ is very large, and rather similar to what is seen in the observational data in the shaded area (0.8–3 $\mathrm{M}_\odot$; Fig. 1). This is interesting, because in these models it is the stars in the mass range 3–9 $\mathrm{M}_\odot$ that are the most massive *and* abundant enough to eject each other from the core after meeting there through mass segregation, causing large fluctuations in the measured MF. The same holds true for the cluster data in the shaded range in Fig. 1. For example, ρ Oph contains not more than a few hundred systems, so that the most massive stars populate roughly the shaded range. The Pleiades is 100 Myr old, so that stars with $m \gtrsim 10\,\mathrm{M}_\odot$ have evolved off the main sequence, and the stars just below this mass interact in the cluster core.

In summary, comparison of the three figures shows that the scatter in α decreases as N increases, but that the scatter is larger than pure Poisson noise (compare the $t > 0$ data in the upper panel of Fig. 9 with the $N = 10^4$ model in Fig. 3). The most important result, though, is that $\alpha_{1,2}$ is underestimated by $\Delta\alpha \approx 0.5$ for the system MF in the mass range 0.1–1 $\mathrm{M}_\odot$. Also, an observer deduces fewer BDs in an unevolved population ($t = 0$; Fig. 4) such as in Taurus–Auriga, than in a population that is older than a few crossing times, such as the Trapezium and the Pleiades clusters (see also Kroupa, Aarseth & Hurley 2001). The figures also show that for a single-age population the scatter is always smaller for $m \lesssim 1\,\mathrm{M}_\odot$. For $m \gtrsim 1\,\mathrm{M}_\odot$, the scatter for the clusters with $N = 3000$ and $N = 10^4$ stars is comparable to the observed scatter. Even when $N = 10^4$, models with $\alpha_3 = 2.3$ cannot be differentiated from models with $\alpha_3 = 2.7$ in mass ranges $b5$ and $b6$.

5.3 The alpha-plot for cluster halo populations

The MF 'in' young rich clusters can often be determined only by avoiding the crowded central regions. This can cause systematic uncertainties, because stellar encounters lead to preferentially lower mass stars and preferentially single stars populating an extended halo, or being ejected from the cluster.

The clusters with $N = 3000$ and $N = 10^4$ stars are used to investigate the MF for systems lying at a distance $R > 3.2$ pc from the cluster centre. The results are shown in Fig. 10, assuming that the observer can only determine the masses of systems.

The scatter is larger than within the clusters ($R \leq 3.2$ pc; Section 5.2), and the bias for $m < 0.5\,\mathrm{M}_\odot$ that leads to an underestimate of α_1 in binary-rich populations is reduced significantly. This results because the halo population is depleted in binary stars (Fig. 5).

Two extreme examples are marked with double symbols. The corresponding MFs are plotted in Fig. 11. One example is the system MF for a halo population at an age of 3 Myr. Its particularly flat MF for $m > 10\,\mathrm{M}_\odot$ ($\alpha = 0.97$) comes about because the

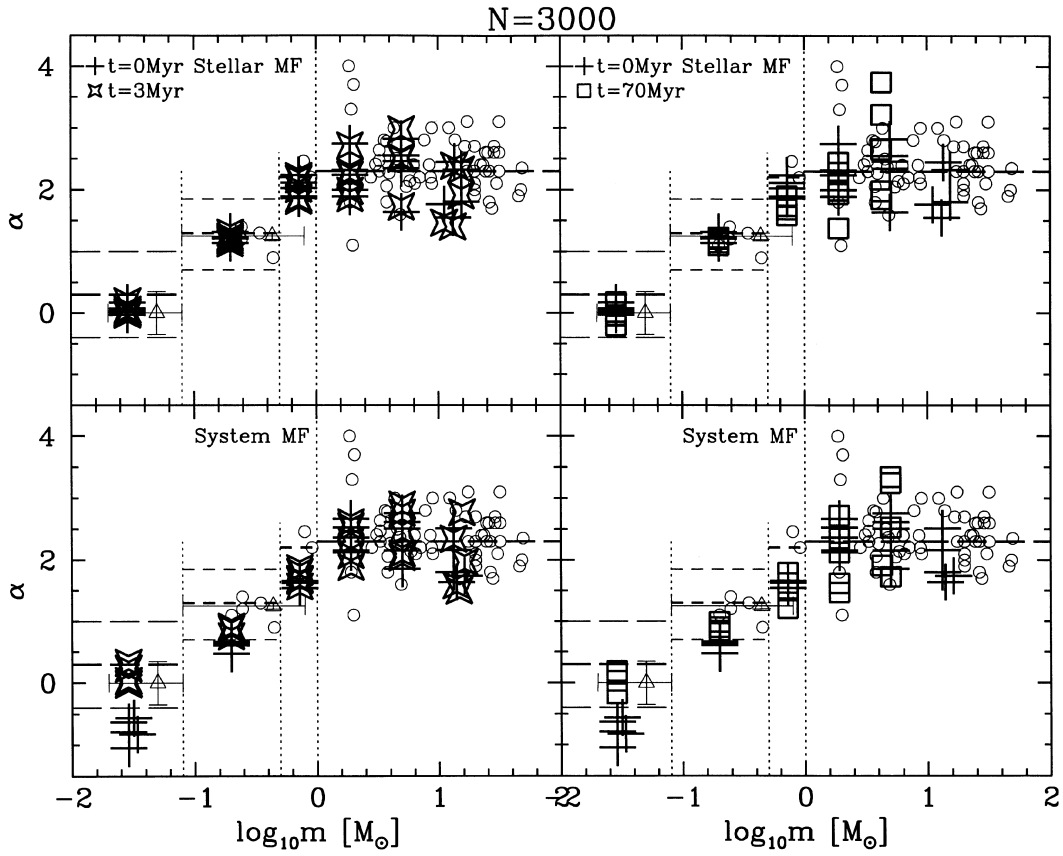

Figure 8. As in Fig. 7, but for five B3000 models.

cluster core just expelled a few massive stars to the outer regions. The steep MF for a 70-Myr-old population with $\alpha = 4.85$ at $\mathrm{l}m_{\mathrm{av}} = 0.9$ (double square in the lower panel) arises because stellar evolution has removed stars with $m \gtrsim 10\,\mathrm{M}_{\odot}$, and because the stars with a mass just below the turn-off mass are located preferably near the cluster core. The fitted power-law indices are listed in Table 3.

5.4 A synthetic alpha-plot

The results from all cluster models at different times and for the inner and outer cluster regions can be combined to form a synthetic ensemble of populations. The result is shown in Fig. 12 for the case that the observer is able to measure the mass of each star exactly. Fig. 13 shows the results assuming that the observer can measure the system masses exactly.

The model α values obtained by fitting power laws to the model system MFs are consistent with $\alpha \approx 2.3$ for $m \gtrsim 1\,\mathrm{M}_{\odot}$, thus rederiving the input IMF despite unresolved binary systems. This result will be revisited in future work for the reasons stressed in Sections 2.1.1 and 4.4.

For $m < 1\,\mathrm{M}_{\odot}$, the average system αs are too small, except in the BD regime, where approximately the input value ($\alpha_0 = +0.3$) is arrived at because of the small surviving binary proportion. Fig. 13 thus demonstrates that the observational data (open circles and triangles) underestimate the single-star power-law index in mass ranges $b2$ and $b3$ (equation 4) by about $\Delta\alpha \approx 0.5$, because binary systems are not resolved. This is a *reliable result*, because of the reasoning in Section 4.4, i.e., because the cluster library used here has an extreme initial density. *Any Galactic embedded cluster with a lower density may lead to a larger bias*, because in lower density clusters the binary population is eroded at a slower rate, allowing a higher binary proportion to survive for longer times. The binary proportion is certainly not lower in such clusters, which is also confirmed by detailed analysis of observations (e.g. Kähler 1999 for the Pleiades; Kroupa & Tout 1992 for Praesepe).

Again it is stressed that the above *corrections to α are minimum values*, especially for BDs. The binary proportion of these may be larger in clusters with lower density, because it takes longer for f_{BD} to decrease in lower density clusters. The maximum corrections to be applied to the observed, i.e., system MFs, are derived from the models at $t = 0$ (e.g. Fig. 9): $\Delta\alpha = +1.3$ for BDs, and $\Delta\alpha = +0.8$ for $0.08 \leq m < 1\,\mathrm{M}_{\odot}$. Such large corrections are, however, unlikely, because $f < 1$ usually (except in Taurus–Auriga; cf. Luhman 2000).

The observational data in Fig. 1 therefore imply a single-star IMF that is steeper than equation (2) for $0.08 \lesssim m \lesssim 1\,\mathrm{M}_{\odot}$ by $\Delta\alpha \approx 0.5$ at least. Thus, for these data the corrected IMF has $\alpha_1 \approx 1.8$ for 0.08–0.5 $\mathrm{M}_{\odot}$, and $\alpha_2 \approx 2.7$ for 0.5–1 $\mathrm{M}_{\odot}$, probably with unchanged α_0 and α_3. The implications of this are discussed in Sections 6.2 and 6.3.

Figs 12 and 13 show that the model scatter in α is similar to that seen in the observational sample. Despite starting in each case with the same IMF, an observer deduces power-law indices that have a scatter of about $\sigma_\alpha = 0.5$ for $m \lesssim 1\,\mathrm{M}_{\odot}$ and $\sigma_\alpha = 1$ for $m \gtrsim 1\,\mathrm{M}_{\odot}$, even if each stellar mass is measured exactly. The finding is thus that the IMF can never be determined more

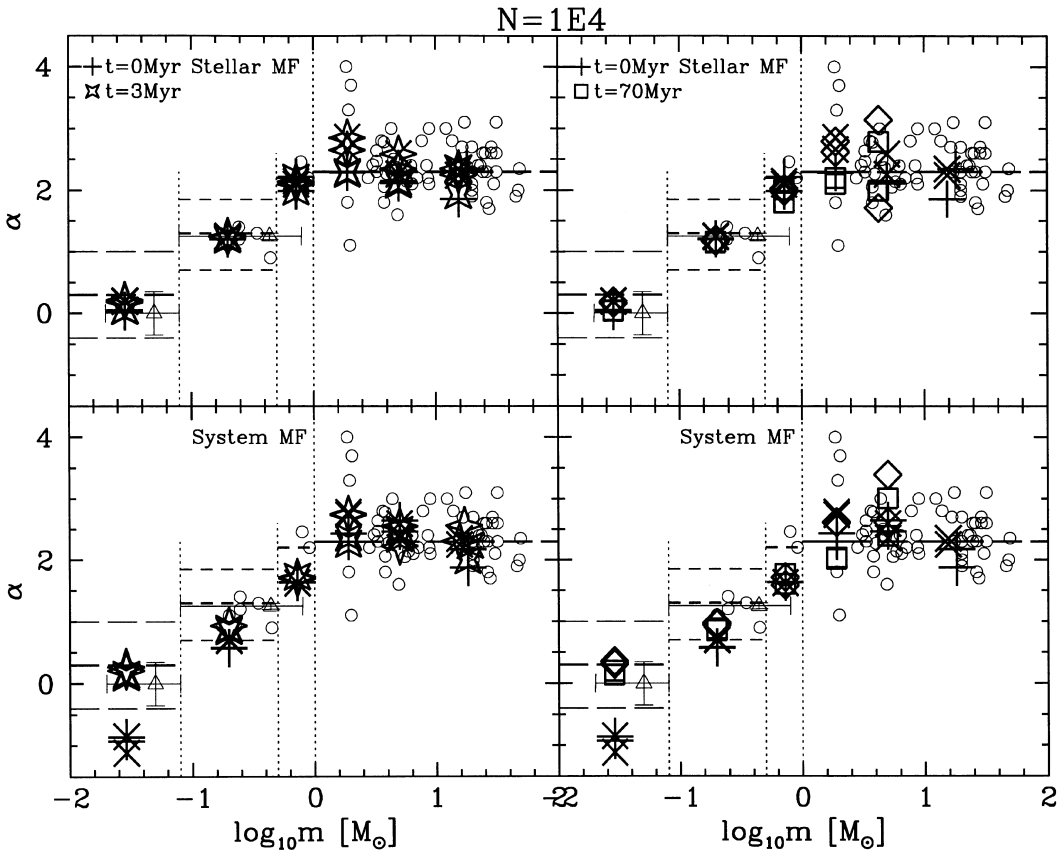

Figure 9. As Fig. 7, but for models with $N = 10^4$ stars. The crosses, four-pointed stars and squares are for the two B1E4 models, whereas the same symbols but rotated by 45° are for the two B1E4d models.

accurately than this scatter, and that the scatter seen in the alpha-plot (Fig. 1) can be explained with Poisson noise and stellar dynamical effects.

6 DISCUSSION

A cautionary remark concerning the alpha-plot is made, namely that in reality the left and right parts of it are disjoint. Also, some tentative evidence *for* a systematically varying IMF is presented, especially in view of the proposed revised IMF.

6.1 The dichotomy problem

When considering the alpha-plot (Fig. 1), it must be remembered that the left ($m \lesssim 1\,M_\odot$) and right ($m \gtrsim 1\,M_\odot$) parts of it are actually disjoint. That is, any nearby cluster that is older than a few Myr, so as to allow the application of reasonably well understood pre-main-sequence or main-sequence stellar models, contains no O stars or is already too old for them to still exist. This is very true for the Galactic-field IMF – there is only an indirect handle on $m \gtrsim 1\,M_\odot$ stars through stellar remnants, but this requires an excellent understanding of stellar evolution, the sfh and Galactic-disc structure (e.g. Scalo 1986). Conversely, any population of stars for which the MF is constrained through observations for $m > 1\,M_\odot$ is usually so far away that the left part of the alpha-plot is not accessible to the observer, and/or so young that measuring the derivative (α), i.e., the *shape* of the IMF for $m < 1\,M_\odot$ becomes a lottery game because of the uncertain pre-main-sequence tracks (Section 1).

That low-mass stars do form in large numbers in any population that also forms O stars *is* established. Examples are the ONC (Hillenbrand 1997), R136 in the 30 Dor region of the LMC (Siriani et al. 2000), and NGC 3603, the most massive visible H II region in the MW (Brandl et al. 1999). However, the ONC is so young that mass estimates become unreliable, compromising conclusions about the detailed shape of its IMF, and in the other cases the census of low-mass stars is not complete. Thus the shape of the IMF spanning $\log_{10} m = -2$ to 2 is not known for *any* population, and it remains an act of faith to assume that the IMF can be approximated by the form of equation (2).

Globular clusters consist entirely of low-mass stars today, but the existence of neutron stars demonstrates that massive stars formed in them as well. Paresce & De Marchi (2000) suggest that the MF for a sample of a dozen globular clusters can be fitted by a log-normal MF with approximately one characteristic stellar mass and standard deviation. A further analysis will show how the differences compare with the spread in α seen in Fig. 1. More interesting in the present context is the fact that Piotto & Zoccali (1999), who use the same stellar models by Baraffe et al. (1997) as Paresce & De Marchi, demonstrate that power-law MFs fit rather well for a wide range of globular clusters, with $\alpha \approx 0.5$–1.2 for $m \lesssim 0.5$–$0.7\,M_\odot$, but the IMF is not measurable for stars with $m \gtrsim 0.7\,M_\odot$.

6.2 A revised IMF

In Section 5.4 the suggestion is made that the systematic bias

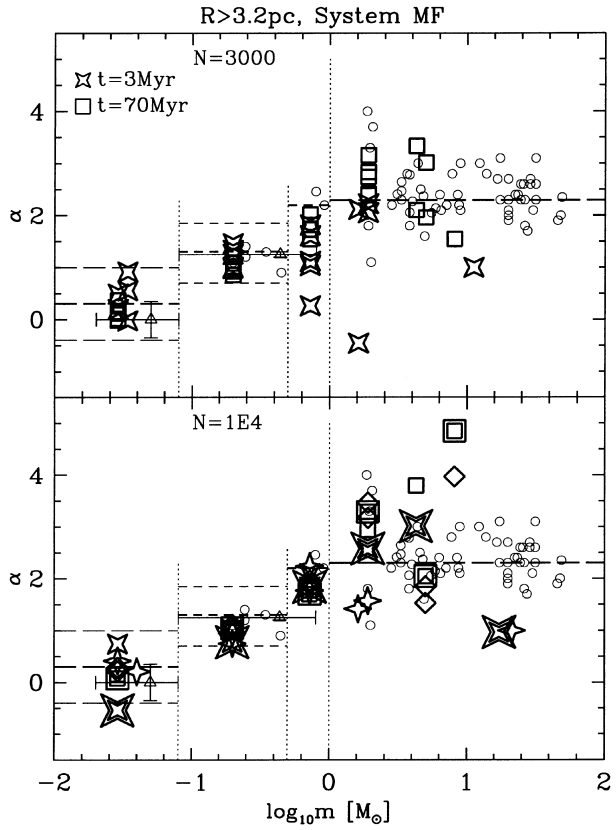

Figure 10. Spatial variation of the MF: The MFs in models B3000 (five renditions), B1E4 (two renditions) and B1E4d (two renditions) for *systems* with $R > 3.2$ pc. Two particularly exotic examples are highlighted using double symbols; the corresponding MFs are plotted in Fig. 11, and the MF fits are listed in Table 3. Otherwise as Fig. 9. Note the changed α-scale.

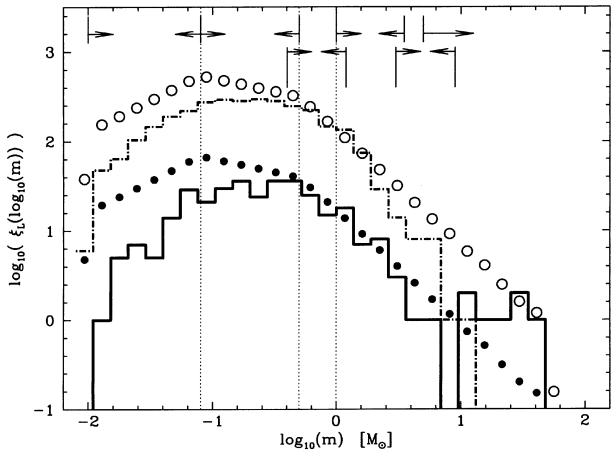

Figure 11. Spatial variation of the MF. The MFs for systems with $R > 3.2$ pc for model B1E4 showing two cases: solid histogram, $t = 3$ Myr (four-pointed double star in Fig. 10) and dot-dashed histogram, $t = 70$ Myr (double square in Fig. 10). The open and filled circles represent the $N = 10^6$ star IMF from Fig. 2 after appropriate scaling. The arrowed mass ranges are as in Fig. 2.

towards low α_1 and α_2 due to unresolved binaries implies that the single-star IMF may be steeper than inferred from observations that do not resolve binary systems. Correcting the ensemble of observed α in Fig. 1 for this bias leads to the following revised

Table 3. The two examples highlighted in Fig. 10. The corresponding MFs are plotted in Fig. 11. The table lists the number of log-mass bins used in the fit, *nb*, the average log-mass over which the fit is obtained, $\log_{10} m_{\rm av}$, the fitted power-law index α, and the probable uncertainty $\sigma_{{\rm f},\alpha}$.

nb	$\log_{10} m_{\rm av}$ [$M_\odot$]	α	$\sigma_{{\rm f},\alpha}$
double star ($t = 3$ Myr) in Fig. 10			
6	−1.540	−0.54	0.31
6	−0.700	+0.77	0.14
4	−0.140	+1.84	0.29
4	+0.280	+2.58	0.54
3	+0.630	+3.01	3.42
6	+1.237	+0.97	1.01
double square ($t = 70$ Myr) in Fig. 10			
6	−1.540	+0.08	0.07
6	−0.700	+1.05	0.05
4	−0.140	+1.70	0.10
4	+0.280	+3.29	0.23
4	+0.700	+2.05	0.69
3	+0.910	+4.85	3.27

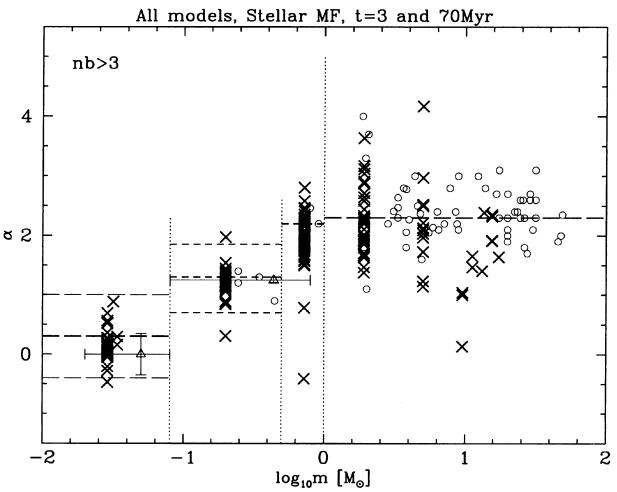

Figure 12. All models B800 (five renditions), B3000 (five renditions) and B1E4 (two renditions) for $t = 3$ and 70 Myr for *individual stars* with $R \leq 3.2$ pc and $R > 3.2$ pc. Only power-law fits that are based on more than $nb = 3$ log-mass bins are plotted. The horizontal and vertical lines, the faint open circles and open triangles have the same meaning as in Fig. 3.

IMF,

$$\begin{aligned}
\alpha_0 &= +0.3 \pm 0.7, \quad 0.01 \leq m/{\rm M}_\odot < 0.08,\\
\alpha_1 &= +1.8 \pm 0.5, \quad 0.08 \leq m/{\rm M}_\odot < 0.50,\\
\alpha_2 &= +2.7 \pm 0.3, \quad 0.50 \leq m/{\rm M}_\odot < 1.00,\\
\alpha_3 &= +2.3 \pm 0.7, \quad 1.00 \leq m/{\rm M}_\odot,
\end{aligned} \tag{6}$$

where the uncertainties from equation (2) are carried over.

The revised IMF has, for stars with $0.01 \leq m \leq 50\,{\rm M}_\odot$, an average stellar mass $\langle m \rangle = 0.20\,{\rm M}_\odot$ and leads to the following population: 50 per cent BDs (0.01–0.08 $M_\odot$) contributing 10 per cent to the stellar mass, 44 per cent M dwarfs (0.08–0.5 $M_\odot$) contributing 39 per cent mass, 4.3 per cent 'K' dwarfs (0.5–1.0 $M_\odot$) contributing 14 per cent mass, 2.3 per cent 'intermediate-mass (IM) stars' (1.0–8.0 $M_\odot$) contributing 24 per cent mass, and 0.15 per cent 'O' stars (>8 $M_\odot$) contributing 12 per cent mass. O and

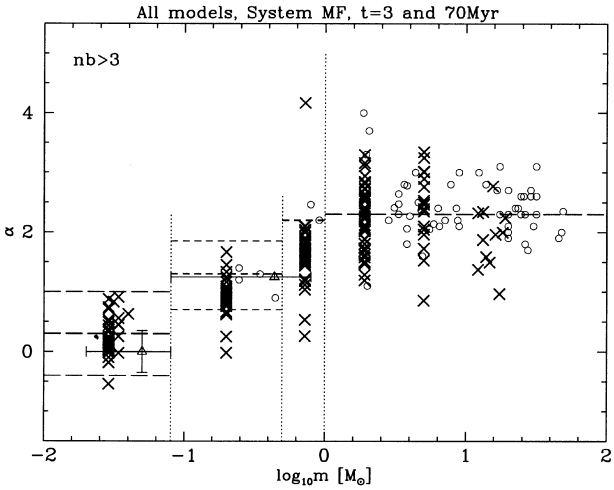

Figure 13. As Fig. 12, but assuming the observer cannot resolve *systems*.

IM stars thus contribute together 36 per cent of the total mass. If $\alpha_4 = 1.15$ ($m > 8\,\mathrm{M}_\odot$), then 50 per cent of the mass is in stars with $8 \leq m \leq 120\,\mathrm{M}_\odot$.

This revised IMF can be viewed as the *present-day star formation IMF*, and is in good agreement with the pre-stellar clump MF measured by Motte et al. (1998) and Johnstone et al. (2000) for ρ Oph: $\alpha_1 \approx 1.5$ and $\alpha_2 \approx 2.5$, especially so since each clump is likely to form a multiple star.

6.3 Possible evidence for a variable IMF

A short account is made of the most promising evidence for a systematically varying IMF. The discussion in Sections 6.3.1 to 6.3.2 is visualized in Fig. 14, in which the various IMFs are compared.

6.3.1 Globular clusters versus Galactic field

The suggestion in Section 6.2 that the alpha-plot (Fig. 1) may imply a present-day star formation (pdsf) IMF (equation 6) that is steeper than the Galactic-field IMF (equation 2) is interesting when compared to the MFs estimated for globular clusters (Section 6.1). These are very ancient and metal-poor systems, so that a systematically different IMF (Larson 1998) ought to be manifest in the data. The difference should be in the sense that globular clusters ought to contain a characteristic stellar mass that is larger than that in more metal-rich populations. The systematically flatter MF in globular clusters compared to the Galactic-field IMF (equation 2), and especially to the pdsf IMF (equation 6), may thus be due to a real difference in the star formation conditions.

However, unfortunately the evidence is not conclusive, because globular clusters have lost preferentially low-mass stars, leading to a systematic flattening of the MF with time, unless the clusters are at large Galactocentric distances (Vesperini & Heggie 1997). The binary proportion in globular clusters is typically smaller ($f \lesssim 0.3$) than in the Galactic field ($f \approx 0.6$), but probably not negligible (Hut et al. 1992; Meylan & Heggie 1997), and correction for their effects may also steepen the measured MF. Approximate corrections that increase the measured α are $\Delta\alpha < 1$ for dynamical evolution (fig. 6 in Vesperini & Heggie 1997) and $\Delta\alpha \approx 0.2$ for unresolved binary systems, but a case-by-case study

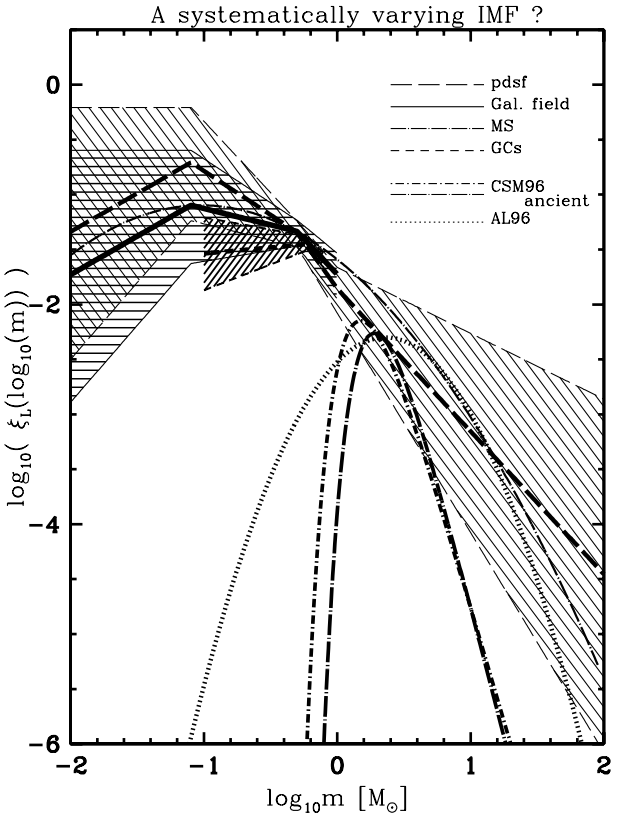

Figure 14. Evidence for a systematically changing IMF. The present-day star formation (pdsf) IMF (equation 6) is shown as the thick dashed line. The Galactic-field IMF (equation 2) is the thick solid line. It is truncated at $m = 1\,\mathrm{M}_\odot$ to express our ignorance about the IMF for $m > 1\,\mathrm{M}_\odot$ for this population that has an average age of about 5 Gyr (the 'dichotomy problem'; Section 6.1). In both cases the shaded areas represent the approximate 95–99 per cent confidence region. For comparison, the Miller & Scalo (1979) log-normal IMF for a constant star formation rate and a Galactic disc age of 12 Gyr is plotted as the thin long-dash-dotted curve (its derivative is shown in Fig. 1). Seven globular clusters give $\alpha_1 = 0.89$, with upper and lower values of 1.22 and 0.53, and $\alpha_2 = 2.3$ for $0.6 < m < 0.8\,\mathrm{M}_\odot$ (Piotto & Zoccali 1999) as indicated by the short-dashed lines and the heavily shaded area. Three possible IMFs for Galactic-halo WD-progenitors are suggested by the thick long-dash-dotted and short-dash-dotted lines (Chabrier, Segretain & Méra 1996, CSM96), and the thick dotted line (Adams & Laughlin 1996, AL96). The MFs have been scaled such that they agree near $0.5\,\mathrm{M}_\odot$, except for the ancient IMFs, which are scaled to fit the Galactic-field IMF near $2\,\mathrm{M}_\odot$.

is required for detailed estimates. In their sample, Piotto & Zoccali (1999) find evidence for flatter MFs at smaller Galactocentric distances, suggesting loss of low-mass stars as being an important bias. However, there is also evidence for a correlation such that more metal-rich clusters have larger α.

The Galactic-field IMF (equation 2) is valid for stars that are, on average, about 5 Gyr old, and which were formed at a different epoch of Galactic evolution than the stars in the clusters featuring in Fig. 1. This, then, suggests a possible systematic shift of star formation towards producing relatively more low-mass stars as star formation moves towards conditions that may favour lower fragmentation masses through higher metallicities and lower cloud temperatures. The fact that the pre-stellar core MF in ρ Oph is somewhat steeper than the Galactic-field IMF (equation 2), while being consistent with a fragmentation origin (Motte et al. 1998), supports this notion.

6.3.2 *Galactic-halo white dwarfs*

Another possible empirical hint for a variable IMF may be provided if part of the dark halo of the Galaxy were in the form of ancient white dwarfs. This is becoming a distinct possibility, given that several candidate ancient halo white dwarfs have been discovered (Elson, Santiago & Gilmore 1996; Ibata et al. 1999, 2000; Méndez & Minniti 2000).

From equation (2) one obtains per WD progenitor (1–8 $M_\odot$; e.g. Weidemann 1990) about eight dwarfs with $m = 0.1$–$0.7\,M_\odot$. No such halo dwarfs that might belong to the same population as the putative WDs have been found, requiring a radically different IMF for their progenitor stars than that seen today in the Galactic disc. Also, for consistency with chemical enrichment data, such an IMF cannot have many stars with $m \gtrsim 5\,M_\odot$ (Adams & Laughlin 1996; Chabrier et al. 1996; Larson 1998; Chabrier 1999).

6.3.3 *Radial variation in a very young cluster*

Hillenbrand (1997) demonstrates that the ONC has pronounced mass segregation, and this may be interpreted as an IMF which has a radial variation, *if* dynamical mass segregation is not fast enough to produce such mass segregation within the age of the cluster. The age of the ONC is estimated to be less than 1 Myr for most ONC stars (Hillenbrand 1997; Palla & Stahler 1999), and Bonnell & Davies (1998) suggest, by using a softened *N*-body code, that mass segregation takes too long to produce the observed effect. However, stellar-dynamical computations with a direct *N*-body code that correctly treats the many close encounters must be applied to this problem (Kroupa, in preparation). If the mass-segregation time-scale is too long to produce the observed effect, then we would have a well-documented case of a variable IMF most likely through interactions of pre-stellar cores, as suggested by Bonnell et al. (1998) and Klessen (2001).

7 CONCLUSIONS

The following three main points are covered in this paper.

I. *The Galactic-field IMF.* The form of the average IMF consistent with constraints from local star-count data and Scalo's (1998) compilation of MF power-law indices for young clusters and OB associations is inferred. The IMF is given by equation (2). This form may be taken as the universally valid IMF.

II. *The alpha-plot: scatter and systematics.* Assuming the universal IMF (equation 2), how large are the apparent variations produced by Poisson noise, the dynamical evolution of star clusters and unresolved binary systems?

This is studied by making use of the alpha-plot, in which IMF power-law indices inferred for *N*-body model populations are plotted as a function of stellar mass. The extreme assumption is made that the observer can measure each stellar or binary-system mass exactly. The resultant *apparent variation* of the IMF thus defines the *fundamental limit for detecting true variations*. Any true variation of the IMF that is smaller than this fundamental limit cannot be detected. This is the reason why no robust evidence for a variable IMF has surfaced to date. The available population samples are too small (e.g., *one* ONC versus *one* ρ Oph).

The model clusters have an initial binary proportion of unity and contain $N = 800$, 3000 and 10^4 stars with a central density as in the ONC. Clusters with a smaller initial density evolve on a longer time-scale. The binary-star problem is thus potentially worse in less dense clusters, because binary systems survive for longer.

The observed spread of power-law indices is arrived at approximately. For the ensemble of model clusters studied here it is $\sigma_\alpha \approx 0.7$ for BDs, $\sigma_\alpha \approx 0.5$ for stars in the mass range 0.1–1 $M_\odot$, and $\sigma_\alpha \approx 1$ for stars with $m \gtrsim 1\,M_\odot$ (Fig. 13).

For stars with $m \gtrsim 1\,M_\odot$, the system MF has, on average, the same power-law index as the underlying single-star IMF. That is, the present models do not lead to any systematic bias in this mass range (but see caveat in Section 2.1.1). Similarly, for BDs the input α is arrived at in the mean, but only if the population is at least a few crossing times old, because by then most BD binaries and star–BD binaries have been disrupted. For a dynamically younger population, α (and the number of BDs) will be underestimated depending on the binary proportion.

To correct for unresolved binaries, the measured power-law index has to be increased by $0 \lesssim \Delta\alpha_0 \lesssim 1.3$ for BDs and $0.5 \lesssim \Delta\alpha_{1,2} \lesssim 0.8$ for $0.08 \leq m \leq 1\,M_\odot$, the upper and lower limits applying for clusters that are unevolved ($t = 0$) and a few crossing times old, respectively, assuming $f = 1$ when $t = 0$. For a population in a cluster that is a few crossing times old, the corrections reduce to $\Delta\alpha_0 \approx 0$ and $\Delta\alpha_{1,2} \approx 0.5$. These corrections have to be applied to any young population to infer the single-star IMF.

Finally, as a cautionary remark, the left and right parts of the alpha-plot are observationally disjoint. It is an act of faith to assume that $\alpha(m)$ has the smooth dependence given by equation (2).

III. *IMF variations.* Applying the above corrections to the ensemble of observed young clusters, a revised (or present-day star formation) IMF is arrived at (equation 6). It is steeper for $m \lesssim 1\,M_\odot$ than the Galactic-field IMF (equation 2), which is a mixture of star formation events with an average age of about 5 Gyr. The pre-stellar clump mass-spectrum in the present-day star-forming cloud ρ Oph (Motte et al. 1998; Johnstone et al. 2000) also indicates a steeper single-star MF than the Galactic-field MF. Intriguingly, the ancient MFs in globular clusters have $\alpha \gtrsim 0$, but closer to zero than the Galactic-field IMF. The recent detection of candidate white dwarfs in the Galactic halo suggests that the IMF of the progenitor population must have been radically different by producing few, if any, low-mass and massive stars ($\alpha \ll 0$ for $m \lesssim 0.5\,M_\odot$ and $\alpha \gg 0$ for $m \gtrsim 2\,M_\odot$).

Furthermore, the well-developed mass segregation in the very young ($\lesssim$2 Myr) ONC may exemplify a locally radially-varying IMF, *if* dynamical mass segregation is too slow. If *N*-body calculations confirm this to be the case (work is in progress), then the ONC will be definite proof that the local conditions determine the average stellar mass, rather than it merely being the result of statistical fluctuations.

The tentative suggestion is thus that some systematic variation may have been detected, with star formation possibly producing relatively more low-mass stars at later Galactic epochs. Such a variation would be expected in the mass range ($\lesssim 1\,M_\odot$) in which turbulent fragmentation, which depends on the cooling rate and thus metal abundance, dominates. Future observations of LMC populations might verify if the IMF has systematically smaller α for $m \lesssim 1\,M_\odot$ than the Galactic-field or present-day star formation IMF. Unfortunately, though, even if there is a trend with metallicity, it will be very arduous to uncover a systematic difference in α between the MW and LMC at low masses, because the metallicity difference is not very large while the α-scatter is. A

lack of systematic differences in α for $m \gtrsim 10\,\mathrm{M}_\odot$ between MW and LMC populations may be a result of one physical mechanism, such as coalescence, dominating in the assembly of massive stars (Larson 1999).

ACKNOWLEDGMENTS

I am grateful to John Scalo for letting me have his compilation of mass function power-law indices, and I thank Sverre Aarseth for making NBODY6 freely available. The *N*-body calculations were performed at the Institut für Theoretische Astrophysik, Heidelberg University, where I spent a few very pleasant years. I acknowledge support through DFG grant KR1635.

REFERENCES

Aarseth S. J., 1999, PASP, 111, 1333
Aarseth S. J., Hénon M., Wielen R., 1974, A&A, 37, 183
Adams F. C., Laughlin G., 1996, ApJ, 468, 586 (AL96)
Allen E. J., Bastien P., 1995, ApJ, 452, 652
Baraffe I., Chabrier G., Allard F., Hauschildt P. H., 1997, A&A, 327, 1054
Bastien P., 1981, A&A, 93, 160
Bonnell I. A., Davies M. B., 1998, MNRAS, 295, 691
Bonnell I. A., Bate M. R., Zinnecker H., 1998, MNRAS, 298, 93
Brandl B., Brandner W., Eisenhauer F., Moffat A. F. J., Palla F., Zinnecker H., 1999, A&A, 352, L69
Briceno C., Hartmann L., Stauffer J., Martin E., 1998, AJ, 115, 2074
Chabrier G., 1999, ApJ, 513, L103
Chabrier G., Baraffe I., 2000, ARA&A, 38, 337
Chabrier G., Segretain L., Méra D., 1996, ApJ, 468, L21
Comeron F., Rieke G. H., Rieke M. J., 1996, ApJ, 473, 294
de La Fuente Marcos R., 1997, A&A, 322, 764
Dominguez I., Chieffi A., Limongi M., Straniero O., 1999, ApJ, 524, 226
Duchene G., 1999, A&A, 341, 547
Duchene G., Bouvier J., Simon T., 1999, A&A, 343, 831
Duquennoy A., Mayor M., 1991, A&A, 248, 485
Eisenhauer F., Quirrenbach A., Zinnecker H., Genzel R., 1998, ApJ, 498, 278
Elmegreen B. G., 1999, ApJ, 515, 323
Elson R. A. W., Santiago B. X., Gilmore G. F., 1996, New Astron., 1, 1
Evans N. R., 1995, ApJ, 445, 393
Figer D. F., et al., 1999, ApJ, 525, 750
Ghez A. M., McCarthy D. W., Patience J. L., Beck T. L., 1997, ApJ, 481, 378
Gilmore G., Howell D., 1998, The Stellar Initial Mass Function. Astron. Soc. Pac., San Francisco
Gilmore G. et al., 1998, in Reasenberg R. D., ed., Proc. SPIE, Astronomical Interferometry, Vol. 3350
Gould A., Bahcall J. N., Flynn C., 1997, ApJ, 482, 913
Haywood M., Robin A. C., Crézé M., 1997, A&A, 320, 428
Heger A., Langer N., 2000, ApJ, 544, 236
Heggie D. C., 1975, MNRAS, 173, 729
Henry T. J., Ianna P. A., Kirkpatrick J. D., Jahreiss H., 1997, AJ, 114, 388
Herbst T. M. et al., 1999, ApJ, 526, L17
Hillenbrand L. A., 1997, AJ, 113, 1733
Hillenbrand L. A., Carpenter J. M., 2000, ApJ, in press
Holtzman J. A. et al., 1997, AJ, 113, 656
Holtzman J. A. et al., 1998, AJ, 115, 1946
Hurley J. R., Pols O. R., Tout C. A., 2000, MNRAS, 315, 543
Hut P. et al., 1992, PASP, 104, 981
Ibata R. A., Richer H. B., Gilliland R. L., Scott D., 1999, ApJ, 524, L95
Ibata R. A., Irwin M., Bienaymé O., Scholz R., Guibert J., 2000, ApJ, 532, L41
Johnstone D. et al., 2000, ApJ, in press
Kähler H., 1999, A&A, 346, 67
Kenyon S. J., Hartmann L., 1995, ApJS, 101, 117
Klessen R., 2001, ApJL, in press
Klessen R. S., Burkert A., 2000, ApJS, 128, 287
Kroupa P., 1995a, ApJ, 453, 358
Kroupa P., 1995b, MNRAS, 277, 1491
Kroupa P., 1995c, MNRAS, 277, 1507
Kroupa P., 1995d, MNRAS, 277, 1522
Kroupa P., 2000a, New Astron., 4, 615
Kroupa P., 2000b, in Lancon A., Boily C., eds, Massive Stellar Clusters, ASP Conf. Ser. Vol. 211. Astron. Soc. Pac., San Francisco, p. 233
Kroupa P., 2001a, in Deiter S. et al., eds, ASP Conf. Ser., STAR 2000: Dynamics of Star Clusters and the Milky Way. Astron. Soc. Pac., San Francisco, in press (astro-ph/0011328)
Kroupa P., 2001b, in Grebel E., Brander W., eds, ASP Conf. Ser., Modes of Star Formation. Astron. Soc. Pac., San Francisco, in press
Kroupa P., Tout C. A., 1992, MNRAS, 259, 223
Kroupa P., Tout C. A., Gilmore G., 1991, MNRAS, 251, 293 (KTG91)
Kroupa P., Tout C. A., Gilmore G., 1993, MNRAS, 262, 545 (KTG93)
Kroupa P., Aarseth S. J., Hurley J. R., 2001, MNRAS, 321, 699
Kurucz R. L., 2000, Proceedings of the Workshop on Nearby Stars, in press (astro-ph/0003069)
Lada C. J., Lada E. A., 1991, in James K., ed., ASP Conf. Ser. Vol. 13, The Formation and Evolution of Star Clusters. Astron. Soc. Pac., San Francisco, p. 3
Larson R. B., 1998, MNRAS, 301, 569
Larson R. B., 1999, in Nakamoto T., ed., Star Formation. Nobeyama Radio Observatory, p. 336
Luhman K. L., 2000, ApJ, 544, 1044
Luhman K. L., Rieke G. H., 1998, ApJ, 497, 354
Luhman K. L., Rieke G. H., 1999, ApJ, 525, 440
Maciel W. J., Rocha-Pinto H. J., 1998, MNRAS, 299, 889
Maeder A., Meynet G., 2000, ARA&A, 38, 143
Martin E. L. et al., 2000, ApJ, 543, 299
Mason B. D. et al., 1998, AJ, 115, 821
Massey P., 1998, in Gilmore G., Howell D., eds, ASP Conf. Ser. Vol. 142, The Stellar Initial Mass Function. Astron. Soc. Pac., San Francisco, p. 17
Massey P., Hunter D. A., 1998, ApJ, 493, 180
Massey P., Lang C. C., Degioia-Eastwood K., Garmany C. D., 1995a, ApJ, 438, 188
Massey P., Johnson K. E., Degioia-Eastwood K., 1995b, ApJ, 454, 151
McCaughrean M. J., Stauffer J. R., 1994, AJ, 108, 1382
Méndez R. A., Minniti D., 2000, ApJ, 529, 911
Meusinger H., Schilbach E., Souchay J., 1996, A&A, 312, 833
Meylan G., Heggie D. C., 1997, A&AR, 8, 1
Miller G. E., Scalo J. M., 1979, ApJS, 41, 513
Motte F., André P., Neri R., 1998, A&A, 336, 150
Muench A. A., Lada E. A., Lada C. J., 2000, ApJ, 533, 358
Murray S. D., Lin D. N. C., 1996, ApJ, 467, 728
Najita J. R., Tiede G. P., Carr J. S., 2000, ApJ, 541, 977
Palla F., Stahler S. W., 1999, ApJ, 525, 772
Paresce F., De Marchi G., 2000, ApJ, 534, 870
Piotto G., Zoccali M., 1999, A&A, 345, 485
Preibisch T., Balega Yu., Hofmann K.-H., Weigelt G., Zinnecker H., 1999, New Astron., 4, 531
Press W. H., Teukolsky S. A., Vetterling W. T., Flannery B. P., 1994, Numerical Recipes. Cambridge Univ. Press, Cambridge
Price N. M., Podsiadlowski Ph., 1995, MNRAS, 273, 1041
Reid I. N., 1991, AJ, 102, 1428
Reid I. N., Gizis J. E., 1997, AJ, 113, 2246
Reid I. N. et al., 1999, ApJ, 521, 613
Rocha-Pinto H. J., Scalo J., Maciel W. J., Flynn C., 2000, A&A, 358, 869
Röser S., 1999, Rev. Mod. Astron., 12, 79
Sagar R., Richtler T., 1991, A&A, 250, 324
Salpeter E. E., 1955, ApJ, 121, 161
Scalo J. M., 1986, Fundam. Cosmic Phys., 11, 1
Scalo J. M., 1998, in Gilmore G., Howell D., eds, The Stellar Initial Mass Function, ASP Conf. Ser., Vol. 142. Astron. Soc., San Francisco, p. 201

Sirianni M., Nota A., Leitherer C., De Marchi G., Clampin M., 2000, ApJ, 533, 203
Terlevich E., 1987, MNRAS, 224, 193
Testi L., Palla F., Natta A., 1999, A&A, 342, 515
Vesperini E., Heggie D. C., 1997, MNRAS, 289, 898
Weidemann V., 1990, ARA&A, 28, 103
Williams D. M., Rieke G. H., Stauffer J. R., 1995a, ApJ, 445, 359
Williams D. M., Comeron F., Rieke G. H., Rieke M. J., 1995b, ApJ, 454, 144
Wuchterl G., Tscharnuter W. M., 2000, A&A, submitted
Zoccali M. et al., 2000, ApJ, 530, 418

This paper has been typeset from a TEX/LATEX file prepared by the author.